

Forest migration outpaces tree species range shift across North America

Akane Abbasi

Purdue University

Christopher Woodall

United States Department of Agriculture, Forest Service

Javier Gamarra

Food and Agriculture Organization of the United Nations <https://orcid.org/0000-0002-1290-9559>

Thomas Ochuodho

Department of Forestry and Natural Resources, University of Kentucky

Sergio de-Miguel

Department of Crop and Forest Sciences, University of Lleida

Rajeev Sahay

School of Electrical and Computer Engineering, Purdue University

Songlin Fei

Purdue University West Lafayette <https://orcid.org/0000-0003-2772-0166>

Alain Paquette

Université du Québec à Montréal <https://orcid.org/0000-0003-1048-9674>

Han Chen

Lakehead University <https://orcid.org/0000-0001-9477-5541>

Ann Christine Catlin

Rosen Center for Advanced Computing, Purdue University

Jingjing Liang (✉ albeka.liang@gmail.com)

Purdue University

Biological Sciences - Article

Keywords: forest migration, migration patterns, North America, tree species range shift

Posted Date: August 23rd, 2021

DOI: <https://doi.org/10.21203/rs.3.rs-840978/v1>

License: © ⓘ This work is licensed under a Creative Commons Attribution 4.0 International License.

[Read Full License](#)

1 **Forest migration outpaces tree species range shift across North America**

2 **Authors:** Akane O. Abbasi¹, Christopher W. Woodall², Javier G. P. Gamarra³, Thomas
3 Ochuodho⁴, Sergio de-Miguel^{5,6}, Rajeev Sahay⁷, Songlin Fei⁸, Alain Paquette⁹, Han Y. H.
4 Chen¹⁰, Ann Christine Catlin¹¹, Jingjing Liang^{1*}

5 **Affiliations:**

- 6 1. Forest Advanced Computing and Artificial Intelligence Lab (FACAI), Department of
7 Forestry and Natural Resources, Purdue University; West Lafayette, Indiana, USA.
- 8 2. United States Department of Agriculture, Forest Service; Durham, New Hampshire,
9 USA.
- 10 3. National Forest Monitoring (NFM) Team, Forestry Division, Food and Agriculture
11 Organization of the United Nations, Rome, Italy.
- 12 4. Department of Forestry and Natural Resources, University of Kentucky; Lexington,
13 Kentucky, USA.
- 14 5. Department of Crop and Forest Sciences, University of Lleida, Lleida, Spain.
- 15 6. Joint Research Unit CTFC – AGROTECNIO – CERCA, Solsona, Spain.
- 16 7. School of Electrical and Computer Engineering, Purdue University; West Lafayette,
17 Indiana, USA.
- 18 8. Department of Forestry and Natural Resources, Purdue University; West Lafayette,
19 Indiana, USA.
- 20 9. Centre for Forest Research, Université du Québec à Montréal; Montréal, Québec,
21 Canada.
- 22 10. Faculty of Natural Resources Management, Lakehead University; Thunder Bay, Ontario,
23 Canada.
- 24 11. Rosen Center for Advanced Computing, Purdue University; West Lafayette, Indiana,
25 USA.

26 * Corresponding author. Email: albeca.liang@gmail.com

27

28

29 **Abstract:**

30 Mounting evidence suggests that geographic ranges of tree species worldwide are shifting under
31 global environmental change, but little is known about forest migration—the shift in the
32 geographic ranges of forest types—and how it differs from individual tree species migration.
33 Here, based on *in situ* records of more than 9 million trees from 596,282 sample plots, we
34 quantified and compared the migration patterns of forests and tree species across North America
35 between 1970 and 2019. On average, forests migrated at a mean velocity of 205.2 km·decade⁻¹,
36 which is twice as fast as species-level migration (95.6 km·decade⁻¹), and 12 times faster than the
37 average of previous estimates (16.3 km·decade⁻¹). Our findings suggest that as subtle
38 perturbations in species abundance can aggregate to change an entire forest from one type to
39 another, failing to see the forest for the trees may result in a gross underestimation of the impacts
40 of global change on forest ecosystem functioning and services. With the first forest classification
41 and quantification of forest migration patterns at a continental level, this study provides an
42 urgently needed scientific basis for a new paradigm of adaptive forest management and
43 conservation under a rapid forest migration.

44

45 **Main text**

46 Trees are immobile organisms, but tree species worldwide are found to undergo
47 substantial changes in geographic distributions under global environmental change. Some tree
48 species move to higher latitudes, tracking warming climate¹⁻⁴, while some move towards lower
49 latitudes^{4,5}, longitudinally⁶, or altitudinally^{7,8}. Collectively, these changes can alter the relative
50 abundance and dominance of tree species, causing a complete change in the type of local forest

51 communities. To differentiate from the term *tree species migration* which refers to the shift of
52 tree species ranges³⁻⁶, we call the shift in the geographic range of a forest type *forest migration*.

53 Quantifying forest migration is crucial for the understanding of the impacts of global
54 change on forest ecosystem functioning and services. A forest constitutes a foundational entity
55 supporting most ecosystem services as well as human culture, customs, economies, and identity⁹⁻
56 ¹². In addition, a forest is a fundamental unit of sustainable forest management¹¹. By shifting
57 local forest types, forest migration can extensively change ecosystem functioning and services¹³⁻
58 ¹⁷, causing massive ecological and socioeconomic impacts worldwide¹⁸. For instance, in the
59 central United States, a diminishing supply of *Quercus alba*, *Q. macrocarpa*, and other white oak
60 species caused by the shifting and shrinking ranges of oak-dominated forests is threatening the
61 bourbon industry¹⁹, a staple of American culture and tradition. Meanwhile, the migration of
62 maple-dominated forests has raised concerns over the sustainability of the maple syrup industry
63 in North America²⁰.

64 To see the forest for the trees is a major challenge in quantifying forest migration.
65 Previous studies found that the geographic ranges of some tree species in North America shifted
66 at a mean velocity of 16.3 km·decade⁻¹, with a range of 0.03 –100.20 km·decade⁻¹ (see
67 Supplementary Table 1). However, because these studies were limited to a local or regional scale
68 with inconsistent migration measurements (*e.g.*, some use marginal shifts, but some use centroid
69 or latitudinal shifts), the patterns of forest migration at a continental scale still remain largely
70 unknown²¹. Moreover, as most reported migration velocities were calculated from species-level
71 shifts, how forest migration differs from tree species migration also remains largely unknown.

72 Here, we systematically quantified, for the first time, forest and tree species migration
73 patterns at a continental scale, based on more than 9 million ground-surveyed tree records from

74 596,282 sample plots. Using these *in situ* data, we classified North American forests into a
75 hierarchical system consisting of eight forest biomes and 51 underlying forest types (Table 1,
76 sans forests in Mexico, Central America, and the Caribbean due to a lack of data). We then
77 quantified the azimuth and velocity of forest migration between 1970–1999 and 2000–2019.
78 Similarly, we quantified the azimuth and velocity of tree species migration across the continent
79 during the same time periods.

80 To quantify forest migration, we first used an established machine learning algorithm to
81 consistently classify all forested areas across the study region into 51 forest types (Table 1, see
82 §**Forest Classification in Methods**). There are 49 forest types in eight biomes in the
83 conterminous United States and Alaska, and 35 forest types in six biomes throughout Canada
84 (Fig. 1, Extended Data Figs. 1, 2). The two countries share a total of six forest biomes. The
85 Boreal Forest (total area 2,462,924 km²) is the largest forest biome shared by the two countries,
86 followed by the Eastern Mixed Forest (644,011 km²). Mediterranean California (59,849 km²)
87 and Southern Plains (547,118 km²) are only distributed in the United States. At the forest type
88 level, black spruce–balsam fir (B-E, 750,121 km²) is the largest forest type shared by the United
89 States and Canada, followed by quaking aspen–balsam fir–paper birch (B-A, 349,949 km²) and
90 jack pine—black spruce (B-C, 294,291 km²). The largest non-boreal forest types shared by the
91 two countries are balsam fir–maple–yellow birch (E-I, 229,088 km²) and subalpine fir—
92 Engelmann spruce (W-K, 203,700 km²).

93 Based on the temporal differences of the range of forest types classified above, we
94 quantified the patterns of forest migration in terms of the velocity and azimuth. Among the 43
95 forest types in eight forest biomes that were present in both periods 1970–1999 and 2000–2019
96 across the continent (Table 1), quaking aspen—balsam fir—paper birch forest (B-A) migrated

107 with the highest velocity at $683.3 \text{ km} \cdot \text{decade}^{-1}$, moving eastward (Table 1, Supplementary Table
108 2). Among the twelve forest types that migrated at a speed between 100 and $440 \text{ km} \cdot \text{decade}^{-1}$,
109 five are in the Eastern Mixed Forest biome (E-A, E-C, E-H, E-J, and E-K), three in the Pacific
110 Coastal Forest biome (W-A, W-B, and W-D), and one in the Western Cordillera (W-J),
111 Mediterranean California (W-Q), Central Forest (E-M), and Boreal Forest biome (B-E),
112 respectively (Fig. 1). The remaining forest types migrated at less than $100 \text{ km} \cdot \text{decade}^{-1}$. In terms
113 of the direction of migration, 16 out of 43 forest types migrated westward, 11 eastward, nine
114 southward, and seven northward in the past 50 years (Table 1). Across the continent, forests
115 migrated at a mean velocity of $205.2 \text{ km} \cdot \text{decade}^{-1}$ (Fig. 2a).

116 At the tree species level, we estimated the geographic range of 150 tree species in North
117 America for the same time period to quantify tree species migration. We found that tree species
118 on average migrated at $95.6 \pm 1.7 \text{ km} \cdot \text{decade}^{-1}$ (Fig. 2b). *Picea sitchensis* had the greatest
119 migration velocity of all the tree species ($504.8 \text{ km} \cdot \text{decade}^{-1}$), followed by *Abies balsamea*
120 ($502.0 \text{ km} \cdot \text{decade}^{-1}$) and *Alnus incana* ($359.4 \text{ km} \cdot \text{decade}^{-1}$). In contrast, *Platanus occidentalis*
121 had the lowest migration velocity ($4.3 \text{ km} \cdot \text{decade}^{-1}$), followed by *Quercus macrocarpa* (4.9
122 $\text{ km} \cdot \text{decade}^{-1}$) and *Celtis laevigata* ($5.3 \text{ km} \cdot \text{decade}^{-1}$) (Supplementary Table 3). Across the
123 continent, we found that tree species migrated at a mean velocity five times greater than the
124 average of previous estimates ($16.3 \text{ km} \cdot \text{decade}^{-1}$, with a range of $0.03 - 100.20 \text{ km} \cdot \text{decade}^{-1}$, see
125 Supplementary Table 1). This difference in species-level migration velocity between current and
126 previous studies can be mainly attributed to the fact that very few boreal species have been
127 covered in previous studies. Because boreal tree species were found here to migrate faster in
128 general, and boreal region constitutes the largest forest biome in North America, a lack of boreal
129 tree species coverage in previous studies has resulted in an underestimation of species-level

120 migration velocity at a continental scale. Nevertheless, for temperate biomes, the species
121 migration velocity estimated here is generally consistent with previous estimates. For instance,
122 we estimated that tree species on average migrated at $81.1 \pm 1.1 \text{ km} \cdot \text{decade}^{-1}$ in the eastern region
123 (Fig. 2b), which is consistent with the previous estimates for eastern United States and Quebec,
124 Canada (Supplementary Table 1).

125 Overall across the continent, forest migrated ($205.2 \text{ km} \cdot \text{decade}^{-1}$, Fig. 2a) more than
126 twice as fast as tree species migration ($95.6 \text{ km} \cdot \text{decade}^{-1}$, Fig. 2b). The velocity was the highest
127 for the Boreal Forest biome, where forest migrated almost three times faster than tree species
128 migration ($335.4 \text{ km} \cdot \text{decade}^{-1}$ vs. $113.4 \text{ km} \cdot \text{decade}^{-1}$) (Fig. 2). We further examined potential
129 drivers behind this geographic trend (Fig. 3a) from among three species diversity measures and
130 15 bioclimate variables. Precipitation seasonality, mean temperature of driest quarter, mean
131 temperature of coldest quarter, and tree species evenness were identified as the most important
132 variables (Extended Data Fig. 3). The ratio of forest migration velocity to tree species migration
133 velocity was positively associated with climate change, an aggregated indicator of temporal
134 changes in the top nine bioclimate variables. In contrast, the ratio was negatively associated with
135 tree species evenness (Fig. 3b).

136 The substantial difference in the velocity of migration between forest type and individual
137 tree species therein can also be attributed to the high sensitivity of forest type classification to
138 changes in the abundance and dominance of underlying tree species. A small, local perturbation
139 in species abundance and/or dominance, which has little impact on the overall shift of the species
140 range, can potentially alter the local forest type and the overall forest migration pattern.

141 Our findings suggest that the impacts of global environmental change on forest
142 ecosystem functioning and services may have been grossly underestimated. Since the mean

143 velocity of forest migration ($205.2 \text{ km} \cdot \text{decade}^{-1}$) estimated here is more than 12 times greater
144 than the average of previous estimates ($16.3 \text{ km} \cdot \text{decade}^{-1}$), the associated impacts of on forest
145 ecosystem functioning and services can be much more profound than previously thought.
146 Because forest ecosystem functioning^{22,23}, productivity²⁴, as well as phenology and population
147 turnover^{25,26} are very sensitive to tree species composition and tree species diversity, subtle
148 changes in relative abundance or relative dominance of tree species can aggregate to affect
149 ecosystem services^{22–24,27} in a snowball effect. For example, in the eastern region, our results
150 show that oak–hickory forest (E-M) and Appalachian oak–pine forest (E-N) migrated at 101.6
151 and $36.8 \text{ km} \cdot \text{decade}^{-1}$, respectively, despite a mere 0.02–0.1% reduction in their ranges (Table 1,
152 Supplementary Table 2). Suppressed fire, land-use change, forest fragmentation, and climate
153 change in this region have increased the proportion of competitive, late-successional mesophytic
154 hardwood species (e.g., *Acer* and *Fagus* spp.), while suppressing fire-dependent xerophytic
155 species (e.g., *Quercus* and *Pinus* spp.)²⁸. This “mesophication” of the central eastern forests has
156 already rendered profound ecological and economic impacts on soil processes, nutrient cycling,
157 wildlife food and habitat, and local timber industry²⁹. Moreover, since existing adaptive forest
158 management regimes are based primarily on individual species range projections and associated
159 environmental and social aspects^{30,31}, it would be difficult for these regimes to fully address the
160 consequences of rapid forest migration. To this end, the quantification of forest classification and
161 associated forest migration patterns provided here can inform decision-making to better support
162 assisted species migration strategies in balancing the deleterious effects of rapid forest
163 migration³².

164 Rapid forest migration at the continental scale has profound economic and social
165 implications. Changes in species mix would affect biophysical and environmental factors that

166 directly or indirectly affect timber supply³³, such as forest productivity²⁴, as well as frequency
167 and severity of forest fires and pest infestations^{34–36}. Forest migration could potentially widen the
168 breadth of timber baskets (*i.e.*, timber procurement radii) associated with wood processing
169 plants, hence increasing transportation costs with downstream financial implications regarding
170 finished forest product prices. Such impacts have significant distributive (welfare) and economy-
171 wide consequences through intersectoral linkages, making local forest industry less self-
172 sustainable and more vulnerable to timber price fluctuations³⁷. Furthermore, the collective
173 human experience (*e.g.*, culture, customs, and identities) of rural communities embedded within
174 these forested landscapes have a strong tie to surrounding forest types. From the Sitka spruce—
175 western hemlock forests in the Pacific Coast to the oak–pine forests along the Appalachians
176 (Table 1), the substantial decline of native forests can threaten the customs, identities, and
177 culture of indigenous³⁸ and other local communities, while jeopardizing the non-timber forest
178 products supply and environmental justice overall³⁹. Rapid forest migration places an urgent call
179 upon human communities, especially rural populations, to adapt their cultural norms and
180 relationships with surrounding forests.

181 Our finding that on average forest migration outpaces tree species range shift by 115%
182 across North America can be attributed to two main factors, namely climate change and tree
183 species evenness (Fig. 3b, Extended Data Fig. 3). Climate change is considered the top driver of
184 forest migration, which impacts the movement, persistence, and competition within and between
185 plant communities^{3,39–41}. In addition to a worldwide temperature increase by about 0.2°C per
186 decade⁴², alterations in precipitation patterns, diurnal timing, seasonal intensity, and season
187 length are also evident across the globe⁴². Consistent with previous studies of smaller geographic
188 scales⁶, we found that climate change accelerates forest migration more than it accelerates tree

189 species migration. In contrast, tree species evenness was found to reduce the difference between
190 forest migration velocity and tree species migration velocity. This complements previous
191 findings that biodiversity and species evenness in particular make forest communities more
192 resilient to climate change^{43,44}.

193 The differed migration patterns between forests and tree species observed here represent
194 a snapshot of a more prominent trend seen across the geological time scale. Forests, because of a
195 high sensitivity to tree species composition changes, have over the millennia exhibited shorter
196 life spans than individual species⁴⁰. While most tree species migrated at relatively low velocities
197 across the continent, others went through substantial fluctuations, such as an 8% reduction in the
198 species range of the hemlocks between 5,400 and 4,800 BP⁴¹. These sudden onsets of species-
199 level range shifts have triggered forest migration across North America over the millennia.
200 Besides climate forcing which is generally seen as the main cause of these changes,
201 anthropocentric disturbances, land use change, invasive species, and associated insect/diseases
202 outbreaks are emerging as a suite of drivers that have permanently changed forest landscapes.
203 For instance, the massive monospecific white pine (*Pinus strobus*) forests that once dominated
204 the northern forests have been replaced by mixed hardwoods, due to extensive logging since the
205 European colonization. During the 20th century, an outbreak of *Cryphonectria parasitica* has
206 destroyed nearly four billion American chestnut (*Castanea dentata*) trees, and completely
207 changed eastern hardwood forests of which American chestnut was a keystone species. This
208 study supports the hypothesis that global environmental change is disrupting forests' adaptive
209 responses to climate change formed since the late Quaternary, and is pushing forests to migrate
210 at an unprecedented rate⁴¹.

211 Our findings depict the first continentally consistent and locally relevant record of forest
212 classification and forest migration patterns. These results contribute fundamental insights into the
213 rapid shifts in tree species assemblage distribution under global environmental change, and their
214 underlying drivers. Our machine-learning analyses reveal strong effects of climate change and
215 species evenness on forest migration patterns, and pinpointed forest communities with an
216 extreme migration velocity, where assisted migration and other adaptive forest management
217 efforts¹⁷ are critical in mitigating biodiversity loss, climate change, and associated socioeconomic
218 impacts. Overall, this study provides an urgently needed scientific basis for a new paradigm of
219 adaptive forest management and conservation, so that effective mitigation and intervention
220 efforts can be developed in response to the rapid forest migration.

221

222 **References**

- 223 1. Boisvert-Marsh, L., Périé, C., & de Blois, S. Shifting with climate? Evidence for recent
224 changes in tree species distribution at high latitudes. *Ecosphere* **5**, 1-33 (2014)
- 225 2. Sittaro, F., Paquette, A., Messier, C., & Nock, C. A. Tree range expansion in eastern North
226 America fails to keep pace with climate warming at northern range limits. *Glob. Change*
227 *Biol.* **23**, 3292-3301 (2017)
- 228 3. Woodall, C. W. et al. An indicator of tree migration in forests of the eastern United States.
229 *Forest Ecol. Manag.* **257**, 1434-1444 (2009)
- 230 4. Woodall, C. W. et al. Selecting tree species for testing climate change migration hypotheses
231 using forest inventory data. *Forest Ecol. Manag.* **259**, 778-785 (2010)

- 232 5. Zhu, K., Woodall, C. W., & Clark, J. S. Failure to migrate: lack of tree range expansion in
233 response to climate change. *Glob. Change Biol.* **18**, 1042-1052 (2012)
- 234 6. Fei, S. et al. Divergence of species responses to climate change. *Science advances*, **3**,
235 e1603055 (2017)
- 236 7. Kelly, A. E., & Goulden, M. L. Rapid shifts in plant distribution with recent climate change.
237 *P. Natl. A. Sci. USA* **105**, 11823-11826 (2008)
- 238 8. Lenoir, J., Gégout, J. C., Marquet, P. A., De Ruffray, P., & Brisse, H. A significant upward
239 shift in plant species optimum elevation during the 20th century. *Science* **320**, 1768-1771
240 (2008)
- 241 9. Food and Agriculture Organization of the United Nations (FAO), & Platform for
242 Agrobiodiversity Research (PAR) *Biodiversity for Food and Agriculture: Contributing to*
243 *Food Security and Sustainability in a Changing World* (FAO & PAR, 2010)
- 244 10. Food and Agriculture Organization of the United Nations (FAO), & United Nations
245 Environmental Programme (UNEP) *The State of the World's Forests 2020. Forests,*
246 *biodiversity and people* (United Nations, 2020)
- 247 11. Genin, D., Aumeeruddy-Thomas, Y., Balent, G., & Nasi, R. The multiple dimensions of rural
248 forests: Lessons from a comparative analysis. *Ecol. Soc.* **18**, 27 (2013)
- 249 12. Watson J. E. M. et al. The exceptional value of intact forest ecosystems. *Nat. Ecol. Evol.* **2**,
250 599-610 (2018)
- 251 13. Neilson, R. P. et al. Forecasting regional to global plant migration in response to climate
252 change. *BioScience* **55**, 749-759 (2005)

- 253 14. Kremen, C., & Merenlender, A. M. Landscapes that work for biodiversity and people.
254 *Science* **362**, 304 (2018)
- 255 15. Wellstead, A., & Howlett, M. Assisted tree migration in North America: policy legacies,
256 enhanced forest policy integration and climate change adaptation. *Scand. J. Forest Res.* **32**,
257 535-543 (2017)
- 258 16. Gitay, H., Suárez, A., & Watson, R. *Climate change and biodiversity* (Intergovernmental
259 Panel on Climate Change, 2002)
- 260 17. Intergovernmental Science-Policy Platform on Biodiversity and Ecosystem Services (IPBES)
261 *Report of the Plenary of the Intergovernmental Science-Policy Platform on Biodiversity and*
262 *Ecosystem Services on the Work of its Sixth Session* (IPBES, 2018)
- 263 18. Hanewinkel, M., Cullmann, D. A., Schelhaas, M. J., Nabuurs, G. J., & Zimmermann, N. E.
264 Climate change may cause severe loss in the economic value of European forest land. *Nat.*
265 *Clim. Change* **3**, 203-207 (2013)
- 266 19. Conrad, A. O. et al. Threats to oaks in the eastern United States: Perceptions and
267 expectations of experts. *J. Forest.* **118**, 14-27 (2020)
- 268 20. Rapp, J. M. et al. Finding the sweet spot: Shifting optimal climate for maple syrup
269 production in North America. *Forest Ecol. Manag.* **448**, 187-197 (2019)
- 270 21. Knott, J. A., Jenkins, M. A., Oswalt, C. M., & Fei, S. Community-level responses to climate
271 change in forests of the eastern United States. *Global Ecol. Biogeogr.* **29**, 1299-1314 (2020)
- 272 22. Loreau, M. Biodiversity and ecosystem functioning: recent theoretical advances. *Oikos* **91**, 3-
273 17 (2000)

- 274 23. Cardinale, B. J. et al. The functional role of producer diversity in ecosystems. *Am. J. Bot.* **98**,
275 572-592 (2011)
- 276 24. Liang, J. et al. Positive biodiversity-productivity relationship predominant in global forests.
277 *Science* **354**, aaf8957 (2016)
- 278 25. Pecl, G. T. Biodiversity redistribution under climate change: Impacts on ecosystems and
279 human well-being. *Science* **355**, eaai9214 (2017)
- 280 26. Zhu, K., Woodall, C. W., Ghosh, S., Gelfand, A. E., & Clark, J. S. Dual impacts of climate
281 change: forest migration and turnover through life history. *Glob. Change Biol.* **20**, 251-264
282 (2014)
- 283 27. Paquette, A., & Messier, C. The effect of biodiversity on tree productivity: from temperate to
284 boreal forests. *Global Ecol. Biogeogr.* **20**, 170-180 (2011)
- 285 28. Nowacki, G. J., & Abrams, M. D. The demise of fire and “mesophication” of forests in the
286 eastern United States. *BioScience* **58**, 123-138 (2008)
- 287 29. Ma, W. et al. Fundamental shifts of central hardwood forests under climate change. *Ecol.*
288 *Model.* **332**, 28-41 (2016)
- 289 30. Iverson, L. R., Prasad, A. M., Peters, M. P., & Matthews, S. N. Facilitating adaptive forest
290 management under climate change: A spatially specific synthesis of 125 species for habitat
291 changes and assisted migration over the eastern United States. *Forests* **10**, 989 (2019)
- 292 31. Millar, C. I., Stephenson, N. L., & Stephens, S. L. Climate change and forests of the future:
293 managing in the face of uncertainty. *Ecol. Appl.* **17**, 2145-2151 (2007)

- 294 32. Renwick, K. M., & Rocca, M. E. Temporal context affects the observed rate of climate-
295 driven range shifts in tree species. *Global Ecol. Biogeogr.* **24**, 44-51 (2015)
- 296 33. Ochuodho, T. O., Lantz, V. A., Lloyd-Smith, P., & Benitez, P. Regional economic impacts of
297 climate change and adaptation in Canadian forests: a CGE modeling analysis. *Forest Policy*
298 *Econ.* **25**, 100-112 (2012)
- 299 34. Flannigan, M. D., Logan, K. A., Amiro, B. D., Skinner, W. R., & Stocks, B. J. Future area
300 burned in Canada. *Climatic Change* **72**, 1-16 (2005)
- 301 35. Lemprière, T. C. et al. *The Importance of Forest Sector Adaptation to Climate Change*
302 (Natural Resources Canada, Canadian Forest Service, Northern Forestry Centre, 2008)
- 303 36. van Wagner, C. E. *Fire behavior in northern conifer forests and shrublands in the Role of*
304 *Fire in Northern Circumpolar Ecosystem* (Wiley, 1983)
- 305 37. Zhou, M. Input substitution and relative input price variability in timber markets. *Can. J.*
306 *Forest Res.* **51**, 339-347 (2021)
- 307 38. Chamberlain, J. L., Emery, M. R., & Patel-Weynand T. *Assessment of Nontimber Forest*
308 *Products in the United States under Changing Conditions* (U.S. Department of Agriculture,
309 Forest Service, Southern Research Station, 2018)
- 310 39. Fleetwood, J. Social justice, food loss, and the sustainable development goals in the era of
311 COVID-19. *Sustainability* **12**, 5027 (2020)
- 312 40. Williams, J. W., Shuman, B. N., Webb III, T., Bartlein, P. J., & Leduc, P. L. Late-Quaternary
313 vegetation dynamics in North America: Scaling from taxa to biomes. *Ecol. Monogr.* **74**, 309-
314 334 (2004)

- 315 41. Davis, M. B., & Shaw, R. G. Range shifts and adaptive responses to Quaternary climate
316 change. *Science* **292**, 673-679 (2001)
- 317 42. The Intergovernmental Panel on Climate Change (IPCC) *Global Warming of 1.5°C. An*
318 *IPCC Special Report on the Impacts of Global Warming Of 1.5°C Above Pre-Industrial*
319 *Levels and Related Global Greenhouse Gas Emission Pathways, In the*
320 *Context Of Strengthening the Global Response to the Threat Of Climate Change, Sustainable*
321 *Development, and Efforts to Eradicate Poverty* (IPCC, 2018)
- 322 43. Chapin Iii, F. S. et al. Consequences of changing biodiversity. *Nature* **405**, 234-242 (2000)
- 323 44. Hisano, M., Searle, E. B., & Chen, H. Y. Biodiversity as a solution to mitigate climate
324 change impacts on the functioning of forest ecosystems. *Biol. Rev.* **93**, 439-456 (2018)

Table 1. Summary of forest types and biomes classified based on the present (2000–2019) and past (1970–1999) forest inventories. Only the top dominant species for each forest type are listed to save space. Forest types with “W-“ belongs to West region, “E-“ to East region, and “B-“ to Boreal region.

Forest biome (present area km ²)	Forest type	Forest type name	Time	Area (km ²)	Mean centroid shift ± se (km·decade ⁻¹)	Direction of shift	Key species (importance value)
Pacific Coastal Forest (249,806)	W-A	Sitka spruce—western hemlock	present	12,959	432.6±0.5	W	<i>Picea sitchensis</i> (155), <i>Tsuga heterophylla</i> (21), <i>Populus balsamifera</i> (7)
			past	28,469			<i>Picea sitchensis</i> (169), <i>Tsuga heterophylla</i> (19), <i>Tsuga mertensiana</i> (4)
	W-B	mountain hemlock—cedar—spruce	present	49,228	270.7±0.2	N	<i>Tsuga mertensiana</i> (123), <i>Chamaecyparis nootkatensis</i> (23), <i>Tsuga heterophylla</i> (9)
			past	54,883			<i>Tsuga mertensiana</i> (151), <i>Picea sitchensis</i> (16), <i>Tsuga heterophylla</i> (15)
	W-C	western hemlock—cedar—spruce	present	120,070	18.2±0.1	S	<i>Tsuga heterophylla</i> (115), <i>Pseudotsuga menziesii</i> (29), <i>Thuja plicata</i> (14)
			past	124,151			<i>Tsuga heterophylla</i> (141), <i>Picea sitchensis</i> (22), <i>Chamaecyparis nootkatensis</i> (8)
W-D	red alder—Douglas-fir	present	41,085	156.8±0.2	N	<i>Alnus rubra</i> (72), <i>Pseudotsuga menziesii</i> (50), <i>Acer macrophyllum</i> (23)	
		past	30,329			<i>Alnus rubra</i> (96), <i>Pseudotsuga menziesii</i> (53), <i>Tsuga heterophylla</i> (15)	
W-E	fir—hemlock	present	26,463			<i>Abies amabilis</i> (111), <i>Tsuga heterophylla</i> (27), <i>Tsuga mertensiana</i> (18)	
W-F	yellow-cedar—hemlock	past	10,522			<i>Chamaecyparis nootkatensis</i> (90), <i>Tsuga heterophylla</i> (40), <i>Tsuga mertensiana</i> (34)	
Western Cordillera (502,547)	W-G	pure and mixed lodgepole pine forest	present	124,573	40.0±0.1	S	<i>Pinus contorta</i> (152), <i>Abies lasiocarpa</i> (10), <i>Pseudotsuga menziesii</i> (9)
			past	100,961			<i>Pinus contorta</i> (158), <i>Pseudotsuga menziesii</i> (12), <i>Abies lasiocarpa</i> (9)
	W-H	Northern Rocky Mountains cedar—larch—hemlock	present	33,435	36.6±0.1	N	<i>Thuja plicata</i> (66), <i>Pseudotsuga menziesii</i> (36), <i>Larix occidentalis</i> (28)
			past	24,925			<i>Thuja plicata</i> (89), <i>Abies grandis</i> (26), <i>Tsuga heterophylla</i> (25)
	W-I	grand fir—Douglas-fir	present	47,490	15.4±0.0	N	<i>Abies grandis</i> (98), <i>Pseudotsuga menziesii</i> (40), <i>Larix occidentalis</i> (13)
			past	40,029			<i>Abies grandis</i> (106), <i>Pseudotsuga menziesii</i> (36), <i>Larix occidentalis</i> (15)
	W-J	aspen-mixed conifer	present	31,435	199.7±0.4	W	<i>Populus tremuloides</i> (139), <i>Abies lasiocarpa</i> (13), <i>Pseudotsuga menziesii</i> (10)
			past	25,466			<i>Populus tremuloides</i> (152), <i>Abies lasiocarpa</i> (12), <i>Pseudotsuga menziesii</i> (11)
	W-K	subalpine fir—Engelmann spruce	present	203,700	19.0±0.1	E	<i>Abies lasiocarpa</i> (107), <i>Picea engelmannii</i> (33), <i>Pinus contorta</i> (18)
			past	155,666			<i>Abies lasiocarpa</i> (125), <i>Picea engelmannii</i> (25), <i>Pinus contorta</i> (17)
W-L	white fir—Douglas-fir—ponderosa pine	present	27,668	40.6±0.2	W	<i>Abies concolor</i> (111), <i>Pseudotsuga menziesii</i> (19), <i>Abies magnifica</i> (13)	
		past	35,361			<i>Abies concolor</i> (109), <i>Pseudotsuga menziesii</i> (28), <i>Pinus ponderosa</i> (14)	
W-M	Engelmann spruce—subalpine fir	present	34,246	75.9±0.2	S	<i>Picea engelmannii</i> (109), <i>Abies lasiocarpa</i> (42), <i>Pinus contorta</i> (13)	
		past	62,889			<i>Picea engelmannii</i> (111), <i>Abies lasiocarpa</i> (41), <i>Pinus contorta</i> (12)	
W-N	whitebark—lodgepole pine—subalpine fir	past	12,349			<i>Pinus albicaulis</i> (120), <i>Abies lasiocarpa</i> (42), <i>Pinus contorta</i> (19)	
W-O	western larch—Douglas-fir	past	40,745			<i>Larix occidentalis</i> (44), <i>Pseudotsuga menziesii</i> (43), <i>Pinus contorta</i> (23)	
Mediterranean California (59,849)	W-P	coastal redwood—tanoak	present	23,266	6.8±0.1	N	<i>Lithocarpus densiflorus</i> (77), <i>Pseudotsuga menziesii</i> (44), <i>Sequoia sempervirens</i> (35)
			past	18,271			<i>Lithocarpus densiflorus</i> (89), <i>Sequoia sempervirens</i> (49), <i>Pseudotsuga menziesii</i> (33)
W-Q	California mixed oak woodland	present	36,583	123.0±0.1	S	<i>Pseudotsuga menziesii</i> (42), <i>Quercus chrysolepis</i> (31), <i>Calocedrus decurrens</i> (25)	
		past	52,385			<i>Pseudotsuga menziesii</i> (45), <i>Quercus kelloggii</i> (21), <i>Calocedrus decurrens</i> (17)	
Coastal-Interior Range (65,438)	W-R	Douglas-fir mixed forest	present	34,915	48.0±0.1	W	<i>Pseudotsuga menziesii</i> (150), <i>Tsuga heterophylla</i> (8), <i>Pinus ponderosa</i> (6)
			past	32,276			<i>Pseudotsuga menziesii</i> (158), <i>Pinus ponderosa</i> (7), <i>Pinus contorta</i> (5)
W-S	ponderosa pine—fir	present	30,524	21.2±0.3	N	<i>Pinus ponderosa</i> (149), <i>Pseudotsuga menziesii</i> (24), <i>Pinus contorta</i> (4)	

			past	27,961			<i>Pinus ponderosa</i> (174), <i>Pseudotsuga menziesii</i> (14), <i>Abies concolor</i> (2)	
Eastern Mixed Forest (644,011)	E-A	red oak mixed hardwood forest	present	56,652	229.5±0.1	E	<i>Quercus rubra</i> (26), <i>Acer rubrum</i> (23), <i>Populus grandidentata</i> (16)	
			past	46,698			<i>Quercus rubra</i> (32), <i>Populus grandidentata</i> (26), <i>Acer rubrum</i> (21)	
	E-B	Great Lakes tamarack—spruce	present	10,091	80.4±0.3	W	<i>Larix laricina</i> (135), <i>Picea mariana</i> (27), <i>Thuja occidentalis</i> (7)	
			past	7,987			<i>Larix laricina</i> (128), <i>Picea mariana</i> (27), <i>Abies balsamea</i> (8)	
	E-C	North-central maple forest	present	80,059	155.0±0.1	E	<i>Acer saccharum</i> (92), <i>Acer rubrum</i> (13), <i>Betula alleghaniensis</i> (11)	
			past	49,747			<i>Acer saccharum</i> (107), <i>Acer rubrum</i> (12), <i>Tilia americana</i> (9)	
	E-D	beech—maple	present	50,902	73.6±0.1	W	<i>Fagus grandifolia</i> (80), <i>Acer saccharum</i> (27), <i>Acer rubrum</i> (19)	
			past	104,869			<i>Fagus grandifolia</i> (60), <i>Acer saccharum</i> (26), <i>Tsuga canadensis</i> (22)	
	E-E	Great Lakes pine forest	present	22,786	86.7±0.2	W	<i>Pinus resinosa</i> (89), <i>Pinus banksiana</i> (33), <i>Quercus ellipsoidalis</i> (10)	
			past	10,353			<i>Pinus resinosa</i> (119), <i>Pinus banksiana</i> (15), <i>Populus tremuloides</i> (12)	
	E-F	red maple—hardwood	present	46,720	12.5±0.1	W	<i>Acer rubrum</i> (101), <i>Quercus rubra</i> (7), <i>Acer saccharum</i> (6)	
			past	61,350			<i>Acer rubrum</i> (98), <i>Populus tremuloides</i> (9), <i>Quercus rubra</i> (8), <i>Acer saccharum</i> (8)	
	E-G	eastern hemlock—maple	present	49,452	37.6±0.1	E	<i>Tsuga canadensis</i> (79), <i>Acer rubrum</i> (25), <i>Fagus grandifolia</i> (11)	
past			27,402	<i>Tsuga canadensis</i> (69), <i>Acer rubrum</i> (27), <i>Acer saccharum</i> (13)				
E-H	northern white-cedar—balsam fir	present	28,370	213.4±0.2	W	<i>Thuja occidentalis</i> (101), <i>Abies balsamea</i> (33), <i>Picea mariana</i> (9)		
		past	37,928			<i>Thuja occidentalis</i> (99), <i>Abies balsamea</i> (31), <i>Picea mariana</i> (10)		
E-I	balsam fir—maple—yellow birch	present	229,088	17.7±0.1	W	<i>Abies balsamea</i> (40), <i>Betula alleghaniensis</i> (30), <i>Acer rubrum</i> (24)		
		past	264,717			<i>Acer saccharum</i> (35), <i>Abies balsamea</i> (32), <i>Betula alleghaniensis</i> (24)		
E-J	eastern white pine—maple	present	37,905	108.8±0.1	W	<i>Pinus strobus</i> (87), <i>Acer rubrum</i> (24), <i>Quercus rubra</i> (10)		
		past	38,080			<i>Pinus strobus</i> (92), <i>Acer rubrum</i> (23), <i>Quercus rubra</i> (9)		
E-K	Great Lakes black ash—poplar	present	9,842	104.5±0.1	E	<i>Fraxinus nigra</i> (77), <i>Populus tremuloides</i> (15), <i>Abies balsamea</i> (14), <i>Acer rubrum</i> (12)		
		past	17,210			<i>Fraxinus nigra</i> (62), <i>Populus balsamifera</i> (29), <i>Populus tremuloides</i> (23)		
E-L	black cherry—maple	present	22,143			<i>Prunus serotina</i> (78), <i>Acer rubrum</i> (20), <i>Fraxinus americana</i> (8)		
Central Forest (414,850)	E-M	oak—hickory	present	58,484	100.6±0.1	E	<i>Quercus alba</i> (49), <i>Acer rubrum</i> (15), <i>Quercus velutina</i> (14), <i>Nyssa sylvatica</i> (10)	
			past	62,119			<i>Quercus alba</i> (49), <i>Carya</i> spp. (25), <i>Quercus velutina</i> (25), <i>Cornus florida</i> (13)	
	E-N	Appalachian oak—pine	present	93,250	36.8±0.1	S	<i>Quercus prinus</i> (46), <i>Acer rubrum</i> (26), <i>Nyssa sylvatica</i> (16), <i>Quercus coccinea</i> (11)	
			past	120,228			<i>Quercus prinus</i> (45), <i>Acer rubrum</i> (24), <i>Nyssa sylvatica</i> (13), <i>Quercus coccinea</i> (12)	
	E-O	mixed oak—hickory	present	78,024	9.6±0.1	S	<i>Quercus stellata</i> (33), <i>Pinus echinata</i> (32), <i>Quercus velutina</i> (16), <i>Quercus alba</i> (12)	
			past	49,986			<i>Quercus stellata</i> (57), <i>Carya</i> spp. (27), <i>Quercus velutina</i> (20)	
	E-P	yellow-poplar—maple	present	112,098	35.0±0.0	E	<i>Liriodendron tulipifera</i> (46), <i>Acer rubrum</i> (21), <i>Acer saccharum</i> (11), <i>Betula lenta</i> (11)	
			past	112,147			<i>Liriodendron tulipifera</i> (30), <i>Carya</i> spp. (15), <i>Cornus florida</i> (15), <i>Acer rubrum</i> (14)	
	E-Q	eastern redcedar—white ash—American elm	present	72,994	89.2±0.1	W	<i>Juniperus virginiana</i> (25), <i>Fraxinus americana</i> (13), <i>Ulmus americana</i> (13)	
			past	68,975			<i>Carya</i> spp. (18), <i>Juniperus virginiana</i> (18), <i>Fraxinus americana</i> (15)	
	Southeastern Plains (547,118)	E-R	slash pine mixed	present	49,073	13.6±0.0	S	<i>Pinus elliotii</i> (154), <i>Pinus taeda</i> (6), <i>Taxodium ascendens</i> (4)
				past	44,838			<i>Pinus elliotii</i> (155), <i>Pinus palustris</i> (7), <i>Pinus taeda</i> (5)
		E-S	loblolly pine—sweetgum	present	118,746	41.2±0.1	W	<i>Pinus taeda</i> (152), <i>Liquidambar styraciflua</i> (10), <i>Quercus nigra</i> (4)
past				150,713	<i>Pinus taeda</i> (123), <i>Liquidambar styraciflua</i> (14), <i>Pinus echinata</i> (8)			
E-T		green ash-mixed floodplain forest	present	47,788	28.2±0.1	N	<i>Fraxinus pennsylvanica</i> (26), <i>Celtis laevigata</i> (14), <i>Acer negundo</i> (13)	
			past	54,381			<i>Fraxinus pennsylvanica</i> (17), <i>Liquidambar styraciflua</i> (15), <i>Carya</i> spp. (12)	
E-U		longleaf mixed pine	present	18,482	29.8±0.1	E	<i>Pinus palustris</i> (98), <i>Pinus clausa</i> (18), <i>Quercus laevis</i> (11), <i>Pinus taeda</i> (11)	
			past	20,539			<i>Pinus palustris</i> (106), <i>Pinus clausa</i> (14), <i>Pinus elliotii</i> (11), <i>Pinus taeda</i> (10)	
E-V			present	57,916	23.9±0.1	W	<i>Nyssa biflora</i> (30), <i>Acer rubrum</i> (15), <i>Magnolia virginiana</i> (15), <i>Pinus elliotii</i> (13)	

	southern lowland mixed forest	past	70,701			<i>Nyssa biflora</i> (27), <i>Magnolia virginiana</i> (17), <i>Taxodium ascendens</i> (16)
E-W	sweetgum—water oak—loblolly pine	present	131,721	22.2±0.1	E	<i>Liquidambar styraciflua</i> (48), <i>Quercus nigra</i> (21), <i>Pinus taeda</i> (21), <i>Acer rubrum</i> (12)
		past	134,061			
E-X	Virginia pine—maple	present	38,640	13.4±0.0	S	<i>Pinus virginiana</i> (50), <i>Acer rubrum</i> (17), <i>Oxydendrum arboreum</i> (11)
		past	43,042			
E-Y	loblolly pine—sweetgum mixed	present	84,752			<i>Pinus taeda</i> (86), <i>Liquidambar styraciflua</i> (25), <i>Quercus nigra</i> (10)
E-Z	shortleaf—loblolly pine	past	55,820			<i>Pinus echinata</i> (87), <i>Pinus taeda</i> (18), <i>Quercus stellata</i> (11), <i>Carya</i> spp. (10)
B-A	quaking aspen—balsam fir—paper birch	present	349,949	683.3±0.1	E	<i>Populus tremuloides</i> (105), <i>Abies balsamea</i> (17), <i>Betula papyrifera</i> (13)
		past	1,104,633			
B-B	paper birch—balsam fir	present	153,236	84.9±0.1	E	<i>Betula papyrifera</i> (59), <i>Abies balsamea</i> (42), <i>Picea mariana</i> (20), <i>Picea glauca</i> (18)
		past	123,495			
B-C	jack pine—black spruce	present	294,291	72.3±0.1	W	<i>Pinus banksiana</i> (118), <i>Picea mariana</i> (40), <i>Populus tremuloides</i> (10)
		past	527,541			
B-D	balsam fir—black spruce	present	200,950	51.6±0.0	S	<i>Abies balsamea</i> (113), <i>Picea mariana</i> (22), <i>Betula papyrifera</i> (17), <i>Picea glauca</i> (11)
		past	222,889			
B-E	black spruce—balsam fir	present	750,121	313.3±0.1	W	<i>Picea mariana</i> (150), <i>Abies balsamea</i> (20), <i>Betula papyrifera</i> (7)
		past	436,470			
B-F	white spruce—lodgepole pine	present	714,379			<i>Picea glauca</i> (105), <i>Pinus contorta</i> (22), <i>Betula neoalaskana</i> (14), <i>Picea mariana</i> (12)

Boreal Forest
(2,462,924)

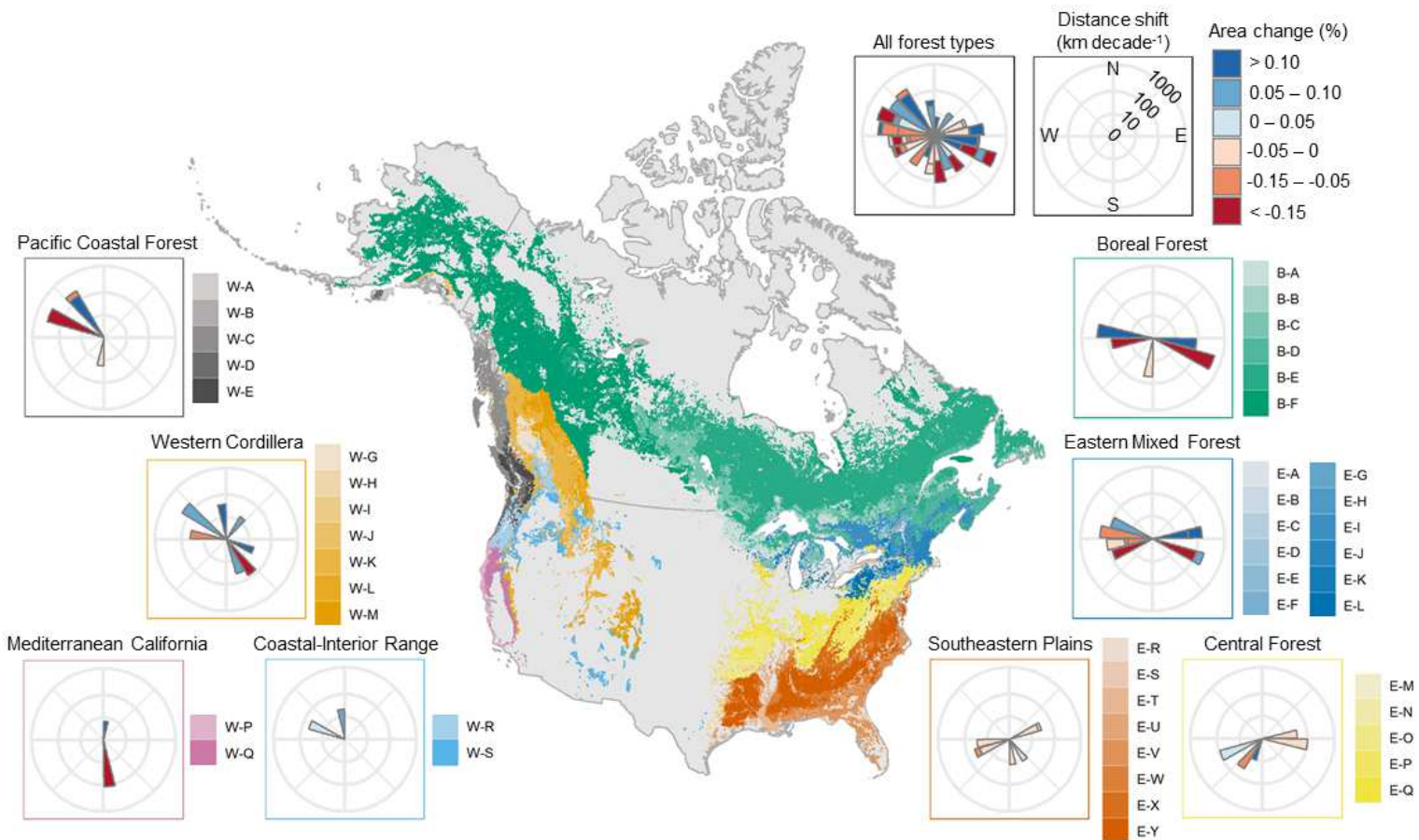


Fig. 1. Map of present (2000–2019) forest type classification, as well as the azimuth and velocity of each forest type. Forest migration was quantified based on the movement of weighted geographic centroids of each forest type. Forest type code corresponds to Table 1.

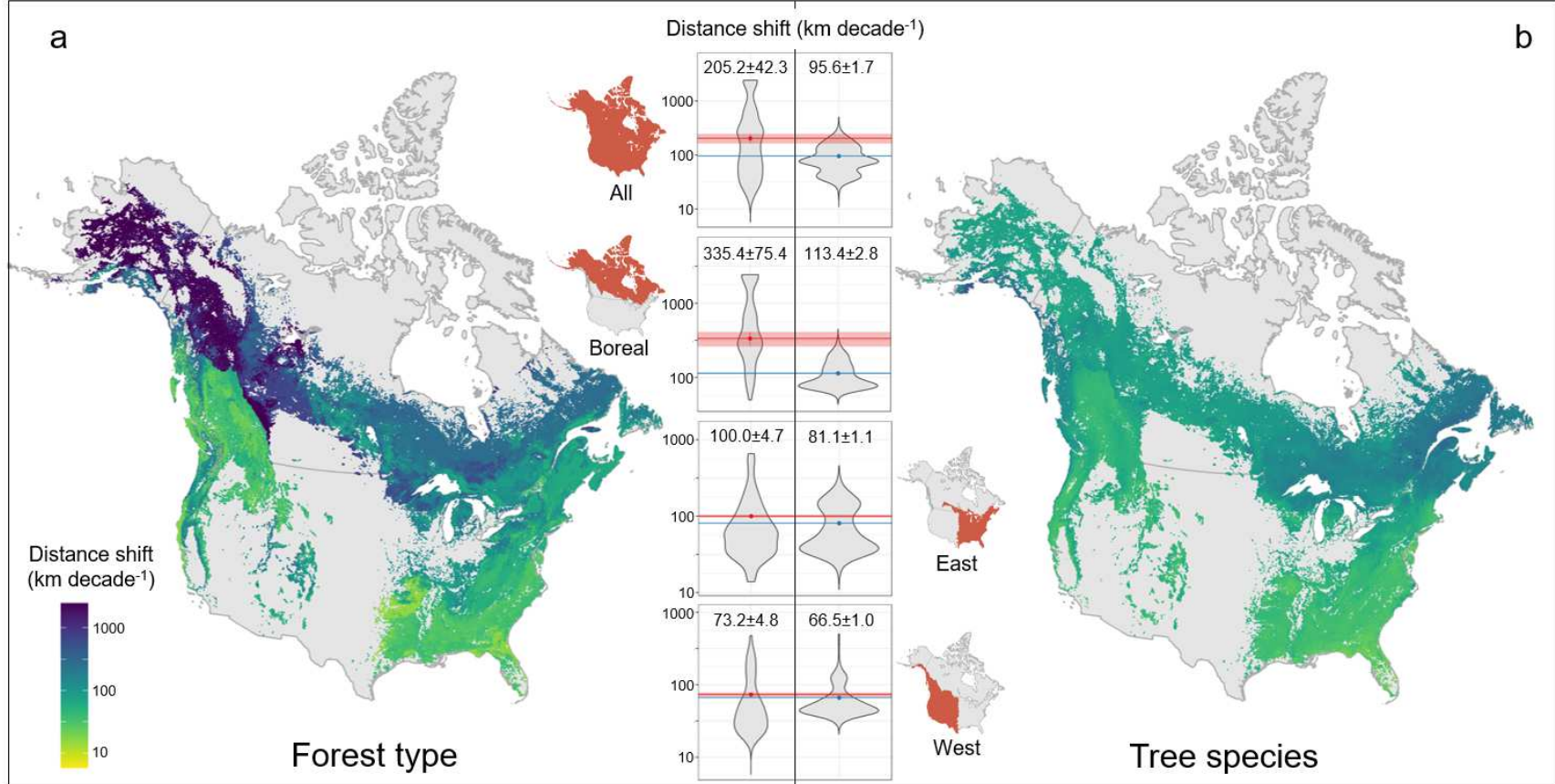


Fig. 2. Comparison of migration velocity (km·decade⁻¹) between forest types (a) and tree species (b), assessed at the 0.025° grid level. Migration velocity was measured by distance shift in kilometers per decade. Violin plots show the distribution of grid-level velocity by region and type (left: forest migration, right: tree species migration). Solid lines and surrounding bands represent the mean and 95% confidence interval, respectively (red represents forest migration velocity, and blue tree species migration velocity).

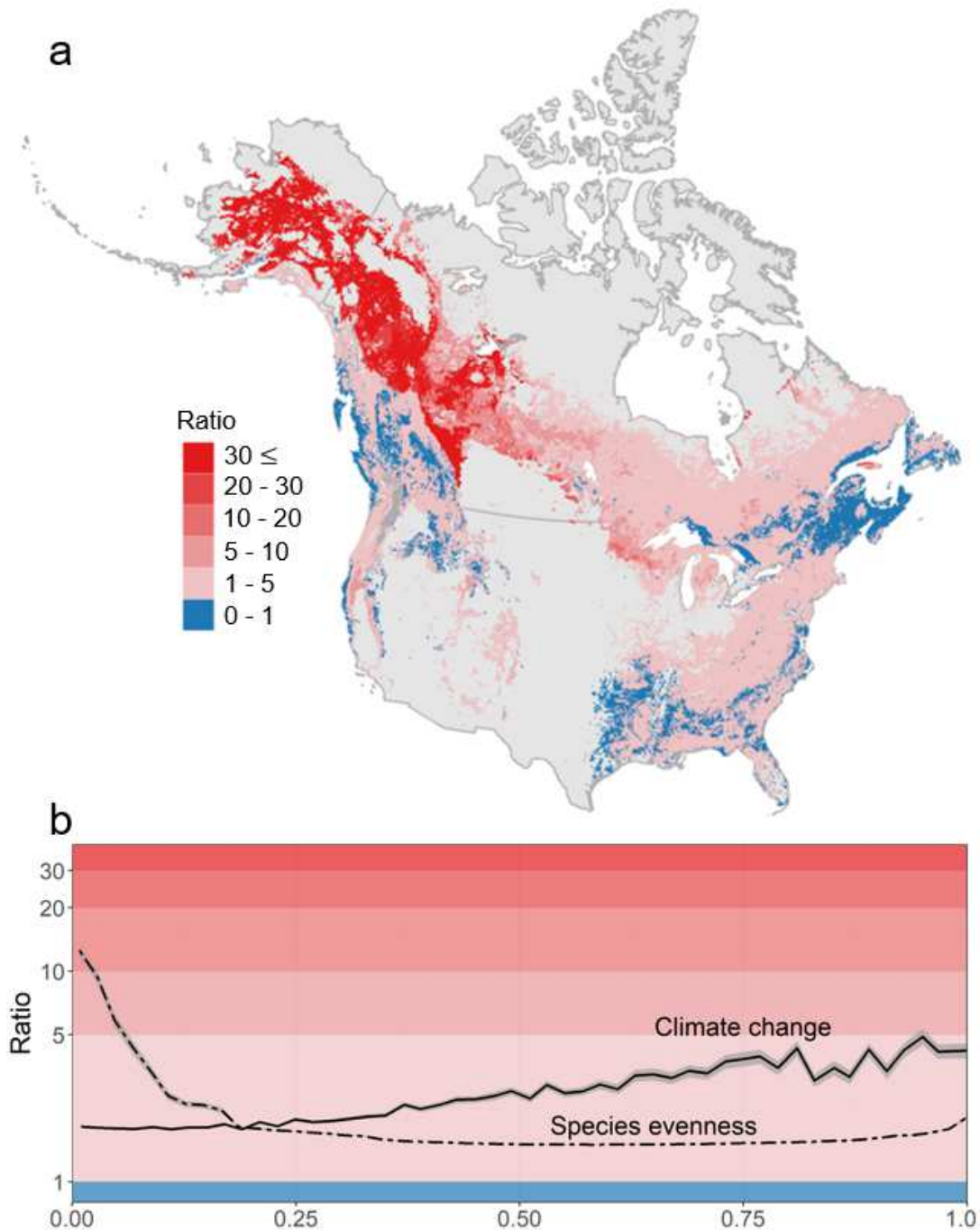


Fig. 3. Geographic distribution and main contributing factors of the ratio of forest migration velocity to tree species migration velocity. In the continental map (a), different colors represent different levels of the ratio and are consistent with background colors of the partial dependence plot (b) which shows the estimated relationship between the ratio and two top contributing variables: climate change and species evenness. Climate change is an aggregated indicator—normalized between 0 and 1—of changes in top nine bioclimate variables ranked by variable importance. Tree species evenness is the average of past (1970-1999) and present (2000-2019) surveys.

Acknowledgments: We thank the Global Forest Biodiversity Initiative (GFBI) for facilitating the international research collaboration. We thank Mo Zhou and John Dunning. Jr. for their feedback on this study.

Funding:

U.S. Department of Agriculture's (USDA) Agricultural Marketing Service through grant AM200100XXXXG007

USDA National Institute of Food and Agriculture McIntire Stennis project 1017711

Start-up Fund provided by the Department of Forestry and Natural Resource and the College of Agriculture, Purdue University

Department of Forestry and Natural Resources, Purdue University

Takenaka Scholarship Foundation (AOA)

Author contributions:

Conceptualization: JL, AOA

Methodology: AOA, JL, RS

Investigation: AOA, JL, CWW, TO

Supervision: JL

Writing – original draft: AOA, JL

Writing – review & editing: All

Competing interests: Authors declare that they have no competing interests.

Methods

Data and data integration

For this study, we compiled and integrated *in situ* forest-tree data from independent and standard forest inventories. Data for the United States came from the Forest Inventory and Analysis (FIA)⁴⁶ and the Cooperative Alaska Forest Inventory (CAFI)⁴⁷. Data for Canada came from two independent sources: permanent sample plot networks^{48,49} and Canada's National Forest Inventory ground plot network⁵⁰. FIA is a nation-wide survey of the extent and status of forests⁴⁶. The plots are permanent sample plots from which data were collected periodically. The FIA plots are approximately 0.1 ha in size and are placed on a hexagonal grid so that there is one plot for every 2,428 ha (6,000 acres) of forested land. In order to maintain the privacy of landowners, all plot coordinates are fuzzed under the passage of the Food Security Act of 1985. However, true coordinates are within 0.80 to 1.61 km of the fuzzed coordinates, so the impact is negligible⁴⁶. CAFI provides a collection of permanent sample plots in southeast Alaska, and the plot size is 0.04 ha in a square shape⁴⁷. The data from permanent sample plot networks of Canada is distributed across eight provinces – British Columbia, Alberta, Saskatchewan, Manitoba, Ontario, Quebec, Nova Scotia, and Newfoundland and Labrador. These plots are 0.04 ha in size, and their distribution over forested areas and re-measurement frequency vary slightly among provinces⁴⁸. The data from Canada's National Forest Inventory ground plot network is distributed across the forested areas in Canada, and plot size differs (125–500 m²)⁵⁰.

We derived the following data integration protocol to harmonize the different forest inventory datasets described above into consistent continental data frames. From each dataset, we obtained tree-level information for all the trees with a minimum diameter at breast height (DBH) of 1 cm. We grouped these tree-level records by the year of inventory, and compiled one

data frame for 2000–2019 and another data frame for 1970–1999. For each period, we then summarized tree-level information into a plot-level species abundance matrix, which contained the percentage of the number of stems by species (*i.e.*, relative abundance), as well as the percent basal area by species (*i.e.*, relative dominance). Based on the species abundance matrix, we calculated the importance value of each tree species present on a sample plot, which equally weights relative abundance and relative dominance of a particular species^{51–53}.

The final continental data frames consisted of plot identification number and coordinates, as well as the importance values of all tree species present on each plot. The plots were uniformly distributed in the sampled areas across the continent (Extended Data Fig. 4). For the 1970–1999 data frame, because some trees in the genera of *Aesculus*, *Amelanchier*, *Carya*, *Crataegus*, *Halesia*, *Malus*, and *Salix* were recorded only to the genus level, we also calculated the importance values of these genera (Supplementary Table 3). Based on the continental data frames, we aggregated plot-level species importance values into a grid-based forest range map to harmonize the past and present survey data. The grid map consisted of 0.025 by 0.025-degree (approximately 3 by 3 km) grids with a minimum 10% canopy cover, in accordance with FAO's definition of 'forest'⁵⁴. Based on the global forest range map⁵⁵, our study region encompassed 1,004,358 grids of forested area across North America, with a total of ~5 million km². The tropical regions of North America, *i.e.* Mexico, Central America, and the Caribbean, were not included in this analysis due to a lack of remeasured *in situ* data. Our study region covered 92 terrestrial ecoregions⁵⁶ across the United States and Canada. These ecoregions were grouped into three distinct regions: West (39 ecoregions), East (33 ecoregions), and Boreal (20 ecoregions, Extended Data Fig. 4).

Forest classification

A lack of consistent classification of forest communities at a continental scale has been a major obstacle to the understanding of the patterns of forest migration. For over a century, forests have been classified based on tree species composition and structural characteristics^{21,51,52,57-59}. Conventional forest classification is manually defined by experts based on the similarity of forest communities in terms of species dominance⁵⁷⁻⁵⁹. With the recent advancement of forest data availability⁶⁰ and computational capacity, new data-driven forest classification schemes minimize subjective biases and exhibit greater accuracy than conventional approaches^{21,51,52}. To this date, however, little has been done to map forest types at a continental scale using a consistent classification scheme.

Our forest classification consists of two steps: defining forest types and mapping them. The definition of forest types was determined by the combination of autoencoder neural network and K-means cluster analysis. Autoencoder neural networks create a compressed representation of the original data, which is more suitable for K-means cluster analysis than the original data. Then, we mapped forest types determined by the K-means cluster analysis to the forested area using machine learning imputation models. Due to the random nature of K-means cluster analysis, we repeated the whole process 20 times to derive the final classification results.

For each region, based on the continental data frame and aggregated grid data described above, we first used an autoencoder neural network to calculate a latent space representation of the original input features⁶¹. Autoencoder neural networks are unsupervised deep learning models, which use the nonlinear generalization of principal component analysis used to reduce dimensions in data^{61,62}. Autoencoders learn to decompose input data into alternate representations using an encoding function, $e: R^n \rightarrow R^k$, and then reconstruct an approximation of the input using a decoding function, $d: R^k \rightarrow R^n$ ⁶³, where the parameters of e and d are

simultaneously optimized. Both the encoding and decoding functions are comprised of one layer or more to perform z operations between the input and model parameters, where z is the number of units in each layer. The result of all z operations in each layer can then be transformed using a non-linear activation function, $\sigma(\cdot)$, to reveal characteristics of the data distribution in an alternate dimensional space⁶¹. This approach provides a more informative data distribution along with the data's reduced dimensionality for efficient data transformations.

In this work, we used the autoencoders' encoding function, $e: R^n \rightarrow R^k$, where $k < n$, to transform the input data into a reduced dimensional representation to conduct K-means cluster analysis. The reduced dimensional representation of the input information improves robust clustering results, and mitigates the computational complexity of the K-means algorithm ($O(n^2)$). We began by constructing a fully connected autoencoder comprised of an input layer (with n units) followed by three fully-connected layers (consisting of 150, $0.75 * n$, and 150 units, respectively) and the n -dimensional output layer. The output of each fully-connected layer was given by $\sigma(x \cdot w + b)$, where $x, w \in R^p$ and $b \in R$ denote the layer's input, the number of units in each layer, and the threshold bias value, respectively. Note that p represents an arbitrary dimensionality of any given layer. The three hidden layers used a linear activation function and the output layer utilized a sigmoid activation function, which is given by $\frac{1}{1+e^{-(x \cdot w + b)}}$. This sigmoid activation function in the output layer made the overall network non-linear while all the three hidden layers utilized a linear activation function. The encoder, e , and the decoder, d , were simultaneously optimized according to $\min_{e,d} \left\| \frac{1}{n} \sum_{i=1}^n (x_i - d(e(x_i))) \right\|^2$ using the Adam optimizer⁶². After training the autoencoder, the output of the second hidden layer was used to

encode the input into its reduced dimensional representation, which was then inputted into the K-means clustering algorithm.

To avoid potential bias caused by insufficient sample sizes, we excluded the species that are present in less than 60 grids (Supplementary Table 3). Based on the reduced dimensional representation, we conducted a K-means cluster analysis to classify forests across North America. We conducted K-means cluster analysis in R (version 4.0.4) using the built-in function “kmeans”⁶⁴. We set the number of starts to 50 and the maximum iterations to 100. Choosing the number of dimensions from the autoencoder neural network and the number of clusters, as well as the evaluation methods are described in §**Model evaluation** below.

With the defined forest types (i.e., clusters) from the 20 repetitions, we manually matched the same forest type by calculating the Euclidean distance in terms of species importance value between all the combinations of forest types generated from the 20 repetitions. When 10 or more repetitions identified the given forest type, we recognized the forest type as a final forest type. Since we classified forest types for three regions separately (West, East, and Boreal), there were potential overlaps of forest types between regions. To identify and merge potential overlaps, we calculated the Euclidean distance of all combinations of the final forest types in terms of species importance value. If a Euclidean distance was less than 60, across-region forest types were merged. One exception was that western aspen-mixed conifer (W-J) and boreal quaking aspen—balsam fir—paper birch (B-A) remained separated due to the large expanse of *Populus tremuloides*.

Mapping of forest types

To map the distribution of forest types across the 4.9 million-km² study region, we considered two candidate imputation models to estimate the underlying forest type of unsampled

grids based on 38 predictor variables. The two candidate models were random forests and support-vector machines. Random forests are a non-parametric ensemble learning approach⁶⁵, which combines a variant of classification trees and an additional level of randomness by bootstrapping sub-data and different sets of predictor variables to mitigate the multicollinearity issues that most statistical models face⁶⁶. We used the “randomForest” package in R with the default hyperparameter setting⁶⁷. Support-vector machines are supervised learning models which construct a hyperplane or set of hyperplanes in a high- or infinite-dimensional space to help analyze data for classification and regression analysis⁶⁸. We used the “e1071” package in R with the default hyperparameter setting⁶⁹. We compared the performance of these two candidate models and selected random forests as the final imputation model (see §**Model evaluation**; Extended Data Fig. 5).

To train candidate models to predict forest type based on local environmental and biophysical conditions, we compiled a total of 38 predictor variables. The predictor variables we compiled consisted of 17 climate variables^{70–72}, 13 topographic variables⁷³, seven soil variables⁷⁴, and human footprint⁷⁵. These predictor variables were derived from open access satellite-based remote sensing and ground-based survey data layers, all of which have a nominal resolution of 1-km. Detailed information of the predictor variables is available in Extended Data Table 1 and Extended Data Fig. 6. We used “Hmisc” package in R to impute missing data in those predictor variables⁷⁶.

Model evaluation

To maximize the clustering performance, we calculated the *silhouette width* to determine the number of dimensions from the autoencoder neural network and the number of clusters. Silhouette width is an indicator of between-cluster heterogeneity⁷⁷. With a range between -1 and

1, positive silhouette width values indicate that a given member of a cluster is closer to its own cluster's centroid than to the nearest cluster's centroid. Negative values indicate that a given member is closer to the nearest cluster's centroid than to the centroid of its own cluster. Generally, higher silhouette width values indicate greater between-cluster heterogeneity. We used the silhouette width to fine-tune hyperparameters for the autoencoder (the number of dimensions) (Extended Data Fig. 7) and K-means cluster analysis (the number of clusters). We calculated silhouette width using the “cluster” package in R⁷⁷. The mean silhouette widths from our K-means cluster analyses were significantly greater than zero for all forest types ($p < 0.001$) in the West for the present dataset. Eighteen out of 19 forest types in the West, 22 out of 26 in the East, and all six forest types in the Boreal region were significantly greater than zero in the mean silhouette width. In summary, 90% of the forest types classified here were significantly distinct from one another in terms of species composition (Supplementary Table 2).

To assess the performance of the imputation model in mapping forest types across the continent, we conducted a rigorous 80/20 cross-validation using bootstrapping. In each iteration, we used stratified sampling to split the entire dataset into the training (80%) and testing (20%) set, and conducted the combination of under-sampling and oversampling of the training set for both random forests and support-vector machines. Stratified sampling was conducted using the “caret” package in R⁷⁸, and under-sampling and oversampling were conducted using the “UBL” package⁷⁹. Based on five random iterations with sample replacement in each of the 20 repetitions, we calculated the 95% confidence interval of classification accuracy, the Kappa statistic, and elements of confusion matrix, as well as predictor variable importance. For each candidate imputation model, the output was a matrix of class probability from five iterations. We

chose the forest type of majority vote from the five iterations, and thus, our final output was a matrix of class probability from the 20 repetitions.

The classification accuracy, Kappa statistic, and elements of confusion matrices were calculated based on the prediction on the testing set in each iteration. Compared with the support vector machine model, random forests model was 10–17% more accurate in terms of overall accuracy and 11–20% more precise in terms of the Kappa statistic (Extended Data Fig. 5). Therefore, we selected random forests as the final imputation model. The confusion matrices based on random forests models were based on the number of cases in class prediction, standardized in percentage (Extended Data Figs. 8, 9). For the present dataset, the coastal redwood—tanoak forest (W-P) had the highest classification accuracy (88%, Extended Data Fig. 8), and the red maple—hardwood forest (E-F) had the lowest accuracy (18%, Extended Data Fig. 8) among all the classes (*i.e.*, forest types).

Quantifying forest migration patterns

We quantified migration patterns of forest type in terms of velocity ($\text{km}\cdot\text{decade}^{-1}$) and azimuth ($^{\circ}$) of the mean geographic movement, as well as changes in area, based on *in situ* forest inventory data aggregated into 0.025 by 0.025-degree grids. The first inventory was conducted between 1970 and 1999 (past inventory), whereas the second inventory was conducted between 2000 and 2019 (present inventory). We ensured past and present forest types matched so that forest migration can be quantified. To do this, we calculated the Euclidean distance of all combinations between past and present forest types in terms of species importance value. Pairs were considered matching when the forest type of minimum distance was the same between the past-and-present pair. For example, if and only if present forest type X's closest past forest type

is Y, and past forest type Y's closest present forest type is also X, they were considered matching.

For each matching pair of past and present forest types, we determined its mean geographic movement and associated 95% confidence interval using a bootstrapping approach with 1,000 iterations. In each iteration, we randomly sampled 80% of past and present data with replacement and quantified the velocity and azimuth of forest migration, based on the past and present centroids of the geographic range of that forest type. The geographic centroid was calculated by weighting the grid geographic coordinates with percent forest type. After mapping forest types across the continent using the imputation random forest models, all the 1,004,358 grids contain a percentage for each forest type as well as the geographic coordinates (latitude and longitude) of that grid's centroid. Percent forest type was determined by how many repetitions, out of 20 repetitions, returned the particular forest type. Geographic centroids for each forest type were then calculated by weighting the geographic coordinates and percentage in that grid with the following equations:

$$\bar{X}_j = \frac{\sum_{i=1}^n w_{ij} X_i}{\sum_{i=1}^n w_{ij}}, \bar{Y}_j = \frac{\sum_{i=1}^n w_{ij} Y_i}{\sum_{i=1}^n w_{ij}}, \quad (1)$$

where \bar{X}_j is the weighted mean longitude of forest type j , \bar{Y}_j is the weighted mean latitude of forest type j , X_i and Y_i are the longitude and latitude for the centroid of grid i , and w_{ij} is the grid cell level percentage of forest type j .

This geographic distance was calculated using the “sp” package in R⁸⁰, while the associated azimuth was determined using the “sfsmisc” package⁸¹. The velocity of forest migration (km·decade⁻¹) was then calculated as the average distance of movement for each forest type (Table 1) per decade. We also determined area coverage of each forest type by weighting

grid area by percent presence of the forest type. Grid area was estimated using the “raster” package in R⁸².

Comparison of forest migration and tree species migration

To directly compare the geographic shift of forest types and tree species, we calculated grid-level velocity for each entity. For forest type, we quantified grid-level velocity of forest migration by weighting the forest type velocity by percent presence of the forest type in each grid. Percent presence of the forest type here was based on how many models, out of five models, returned the given forest type. Therefore, the output was a matrix of grid-level velocity from the 20 repetitions.

We estimated tree species migration in a similar manner, using the same grid-level forest-tree data for identical time periods. For each tree species and each time period, we estimated tree species distribution range based on random forests models and the 38 predictor variables (Extended Data Table 1). For each region (West, East, and Boreal), only species with sufficient sample size (≥ 60 grids) in both time periods were included (Supplementary Table 3). Following Iverson et al. (2019), we reported the mean predicted importance value for each species or zero for species with zero median and a coefficient of variation no less than 2.75 among all predicted values⁵³. We calculated weighted mean geographic centroids using predicted importance value, and determined the species’ mean geographic shift using the identical method to the one stated above. We then repeated this process 20 times to derive the mean and 95% confidence interval of tree species migration velocity. To maximize the model performance while minimizing computational time, we selected the number of trees = 100 after fine-tuning using the West present dataset as an example. Specifically, we calculated root mean square error (RMSE) for

different number of trees with 10 iterations, and chose the number of trees where RMSE values converged.

Modeling the ratio of forest migration velocity to tree species migration velocity

Based on the grid-level velocities of forest types and tree species, we took the ratio of forest migration velocity to tree species migration velocity for each grid. We then trained a random forests regression model with the ratio being the response variables, and 18 predictor variables (Extended Data Fig. 3). Based on grid-level tree species abundance data, we calculated three biodiversity measures: species richness, Shannon's index, and species evenness. Species richness (S) represents the total number of tree species present in the grid. Shannon's diversity index (H)⁸³ was calculated using the formula:

$$H = - \sum_{i=1}^S p_i \ln p_i, \quad (2)$$

where p_i is the proportion of importance value of species i relative to the sum of importance value of all species present in that grid. Species evenness (E) was calculated using the measure proposed by Chao and Ricotta⁸⁴:

$$E = \frac{e^H - 1}{S - 1}. \quad (3)$$

In addition, we calculated the temporal changes of 15 bioclimate variables (C_1 - C_{15} , Extended Data Table 1) between the past and present surveys, and added these variables ($\Delta C_1, \Delta C_2, \dots, \Delta C_{15}$) as predictor variables. With the total of 18 predictor variables, we conducted a bootstrapping of 100 random forests regression models, each trained with a random 80% subset of the full dataset with replacement. Variable importance was determined based on the Gini impurity, a measure that represents the probability of incorrect classification of randomly selected sample due to its distribution.

Finally, we assessed the partial dependence of the ratio on the predictors with the highest variable importance values, by plotting the predicted ratio values over the range of the predictor variable, holding other variables constant at their sample mean. For all temporal change-related bioclimate variables, we developed climate change as an aggregated indicator, which was calculated as the mean of the top nine most important bioclimate variables normalized to a common range between 0 and 1. We chose to calculate the climate change indicator based on the top nine most important bioclimate variables, because this subset of variables accounted for 68.4% of the total importance values of all the 21 bioclimate variables studied here.

Data and Code availability

All data, code, and materials used in the analysis will be deposited to Figshare and Purdue University Research Repository (PURR) upon the publishing of this paper.

Additional References

46. Burrill, E. A. et al. *The Forest Inventory and Analysis Database: Database Description and User Guide Version 8.0 for Phase 2* (U.S. Department of Agriculture, Forest Service, 2018)
47. Malone, T. Liang, J. & Packee, E. C. *Cooperative Alaska Forest Inventory* (Boreal Ecology Cooperative Research Unit, Pacific Northwest Research Station, U.S. Department of Agriculture, Forest Service, 2009)

48. Chen, H. Y., Luo, Y., Reich, P. B., Searle, E. B., & Biswas, S. R. Climate change-associated trends in net biomass change are age dependent in western boreal forests of Canada. *Ecol. Lett.* **19**, 1150-1158 (2016)
49. Paquette, A., & Messier, C. The effect of biodiversity on tree productivity: from temperate to boreal forests. *Global Ecol. Biogeogr.* **20**, 170-180 (2011)
50. Zhang, Y., Chen, H. Y., & Taylor, A. R. Positive species diversity and above-ground biomass relationships are ubiquitous across forest strata despite interference from overstory trees. *Funct. Ecol.* **31**, 419-426 (2017)
51. Dyer, J. M. Revisiting the deciduous forests of eastern North America. *BioScience* **56**, 341-352 (2006)
52. Costanza, J. K., Coulston, J. W., & Wear, D. N. An empirical, hierarchical typology of tree species assemblages for assessing forest dynamics under global change scenarios. *PloS One* **12**, e0184062 (2017)
53. Iverson, L. R., Peters, M. P., Prasad, A. M., & Matthews, S. N. Analysis of climate change impacts on tree species of the eastern US: Results of DISTRIB-II modeling. *Forests* **10**, 302 (2019)
54. Food and Agriculture Organization of the United Nations (FAO) *Global forest resources assessment 2015 – How are the world's forests changing?* (FAO, 2015)
55. Hansen, M. C. et al. High-resolution global maps of 21st-century forest cover change. *Science* **342**, 850-853 (2013)

56. Olson, D. M. et al. Terrestrial Ecoregions of the World: A New Map of Life on Earth: A new global map of terrestrial ecoregions provides an innovative tool for conserving biodiversity. *BioScience* **51**, 933-938 (2001)
57. Eyre, F. H. *Forest cover types of the United States and Canada* (Society of American Foresters, 1980)
58. Küchler, A. W. *Potential natural vegetation of the conterminous United States* (American Geographical Society, 1964)
59. Rowe, J. S. *Forest regions of Canada* (Department of the Environment, Canadian Forestry Service, 1972)
60. Liang, J., & Gamarra, J. G. The importance of sharing global forest data in a world of crises. *Sci. Data* **7**, 1-5 (2020)
61. Song, C., Huang, Y., Liu, F., Wang, Z., & Wang, L. Deep auto-encoder based clustering. *Intell. Data Anal.* **18**, S65-S76 (2014)
62. Hinton, G. E., & Salakhutdinov, R. R. Reducing the dimensionality of data with neural networks. *Science* **313**, 504-507 (2006)
63. Goodfellow, I., Bengio, Y., Courville, A. *Deep learning* (MIT Press, 2016)
64. R Core Team *R: A language and environment for statistical computing* (R Foundation for Statistical Computing, 2021)
65. Breiman, L. Random forests. *Mach. Learn.* **45**, 5-32 (2001)
66. James, G., Witten, D., Hastie, T., & Tibshirani, R. *An introduction to statistical learning with applications in R* (Springer, 2013)

67. Liaw, A., & Wiener, M. Classification and regression by randomForest. *R News* **2**, 18-22 (2002)
68. Cortes, C., & Vapnik, V. Support-vector networks. *Mach. Learn.* **20**, 273–297 (1995)
69. Meyer, D. et al. Misc functions of the Department of Statistics, Probability Theory Group (Formerly: E1071), vol. R package version 1.7-4. (2020)
70. Fick, S. E., & Hijmans, R. J. WorldClim 2: new 1-km spatial resolution climate surfaces for global land areas. *Int. J. Climatol.* **37**, 4302-4315 (2017)
71. Karger, D. N. et al. Climatologies at high resolution for the earth's land surface areas. *Sci. Data* **4**, 1-20 (2017)
72. Trabucco, A., & Zomer, R. Global Aridity Index and Potential Evapotranspiration (ET0) Climate Database v2. figshare. Fileset <https://doi.org/10.6084/m9.figshare.7504448.v3> (2019)
73. Amatulli, G. et al. A suite of global, cross-scale topographic variables for environmental and biodiversity modeling. *Sci. Data* **5**, 1-15 (2018)
74. Batjes, N. World soil property estimates for broad-scale modelling (WISE30sec). (ISRIC-World Soil Information, 2015).
75. Venter, O. et al. Sixteen years of change in the global terrestrial human footprint and implications for biodiversity conservation. *Nat. Commun.* **7**, 1-11 (2016)
76. Harrell Jr., F. E. Harrell miscellaneous. R package version 4.4-2. (2020)
77. Maechler, M., Rousseeuw, P., Struyf, A., Hubert, M., & Hornik, K. Cluster: Cluster Analysis Basics and Extensions. vol. R package version 2.1.0. (2019)

78. Kuhn, M. et al. Classification and regression training. R package version 6.0-86. (2020)
79. Branco, P., Ribeiro, R., & Torgo, L. An implementation of re-sampling approaches to utility-based learning for both classification and regression tasks. R package version 0.0.6. (2017)
80. Pebesma, E. J., & Bivand, R. S. Classes and methods for spatial data in R. *R News*, **5**, 9-13 (2005)
81. Maechler, M. et al. Utilities from “Seminar fuer Statistik” ETH Zurich. R package version 1.1-8. (2021)
82. Hijmans, R. J. et al. Geographic data analysis and modeling. R package version 3.4-5. (2020)
83. Shannon, C. E. A mathematical theory of communication. *Bell Syst. tech.* **27**, 379-423 (1948)
84. Chao, A., & Ricotta, C. Quantifying evenness and linking it to diversity, beta diversity, and similarity. *Ecology* **100**, e02852 (2019)
85. Iverson, L. R., Prasad, A. M., Matthews, S. N., & Peters, M. Estimating potential habitat for 134 eastern US tree species under six climate scenarios. *Forest Ecol. Manag.* **254**, 390-406 (2008)
86. Zolkos, S. G. et al. Projected tree species redistribution under climate change: implications for ecosystem vulnerability across protected areas in the Eastern United States. *Ecosystems* **18**, 202-220 (2015)
87. Hernández, L., Cañellas, I., Alberdi, I., Torres, I., & Montes, F. Assessing changes in species distribution from sequential large-scale forest inventories. *Ann. For. Sci.* **71**, 161-171 (2014)

Supplementary Files

This is a list of supplementary files associated with this preprint. Click to download.

- [ForestMigrationSITable1final.xlsx](#)
- [ForestMigrationSITable2final.xlsx](#)
- [ForestMigrationSITable3final.xlsx](#)
- [ForestMigrationExtendedData.docx](#)